Arabian Journal for Science and Engineering (2024) 49:261–271
https://doi.org/10.1007/s13369-023-07987-3

RESEARCH ARTICLE-CHEMISTRY

High Adsorption Capacity of Ammonia Gas Pollutant Using Adsorbents of Carbon Composites

Elham F. Mohamed[1] · Asmaa El-Mekawy[1] · Sohair A. Sayed Ahmed[2] · Nady A. Fathy[2]

Received: 12 November 2022 / Accepted: 17 May 2023 / Published online: 26 June 2023

Abstract

Air pollution is one of the most environmentally harmful to the human health and the climate change. The present study is aimed to investigate the effectiveness and capability of novel composite adsorbents prepared from modification of activated carbons (ACs) in the removal of air pollutants. The effect of both triethoxysilane propylamine (TEPSA) and carbon nanotube (CNT) on the adsorption properties of AC (TEPSA/CNT/AC); in addition, silica gel prepared from TEPSA to form silica nanoparticles (SiNP) along with CNT and AC (SiNP/CNT/AC), was studied. Ammonia gas (NH_3) was used in this study as a typical emerging gas air pollutant. The physicochemical characteristics of the prepared ACs samples were analyzed using BET surface area, SEM, EDX, TEM and FTIR. Their results proved considerable changes in the porosity and surface functional groups after modifying AC surface with TEPSA or SiNP and CNT instantly. The adsorption findings showed that the NH_3 removal efficiency using the prepared AC samples reached almost 97, 86 and 75% during 90 min at 25 °C for each sample of SiNP/CNT/AC, TESPA/CNT/AC and AC, respectively. Adsorption of NH_3 relied mainly on the presence of silica particles and mesopore distributions in CNT rather than large total surface area in AC alone. Thus, the combination of SiNP as silanol and siloxane groups with CNT on AC surface raised significantly the adsorption capacity of NH_3 from 194 to 300 mg/g. Conclusively, the SiNP/CNT/AC sample exhibited the best performance among all prepared samples used for the adsorption of NH_3 gas from the indoor air. Also, Langmuir and Freundlich models were applied, and the results revealed that Freundlich model fits well the equilibrium adsorption data.

Keywords Air pollution · Adsorption · Activated carbon-based adsorbents · Ammonia

1 Introduction

Air pollution is one of the major environmental problems that cause health and climate risks. It is closely associated with the health of all living beings such as plants, human and animals. Among the gaseous pollutants, ammonia (NH_3) exists in both outdoor and indoor air, which provokes the harmful to the health and productivity of living creatures. By controlling the air pollutant level, countries can decrease their diseases and then reduce the air pollution economic effect. The majority of NH_3 comes mainly from the activities of agriculture, such as fertilizer industries, combustion of fossil fuel and the management of livestock. Moreover, NH_3 in the indoor air is much higher than that in outdoor, which is essentially generated from the smoke of cigarettes, building materials and the solutions of cleaning [1, 2]. Reducing the pollutants emitted from the sources can augment the efforts to control the climate change impacts, while treating the pollutants can result in air quality improvement. By creating new and highly efficient materials for the removal of pollutants, countries could be capable of protecting health and reducing the global climate change. Several techniques have been supposed in the literature for NH_3 removal from waste gas effluents [3–5]. These include absorption by solution, reaction with other gases, ion exchange using polymeric resins, separation using membranes, thermal treatment, catalytic decomposition and adsorption by porous solids [1, 6]. Among these, adsorption of ammonia using activated carbons (ACs) is one of the efficient approaches used in the

✉ Nady A. Fathy
fathyna.77@hotmail.com

1 Air Pollution Department, Environment and Climate Change Research Institute, National Research Centre, 33 EL Buhouth St., P.O. 12622, Dokki, Giza, Egypt

2 Physical Chemistry Department, Research Institute of Advanced Materials Technology and Mineral Resources, National Research Centre, 33 EL Buhouth St., P.O. 12622, Dokki, Cairo, Egypt

literature because of certain advantages of ACs, such as high surface area, porosity and its surface chemical composition, which can undergo certain modifications to a specific application [7–9]. However, the previous works have shown that the surface chemistry is the most important factor in determining the overall adsorption capacity of ACs for a basic molecule like ammonia [9–12]. Kim et al. [10] found that not only the amount but also the nature of the oxygen surface groups present on the carbon surface, i.e. acidic groups, are responsible mainly for increasing the adsorption of ammonia. Moreover, several studies indicate that the adsorbent surface is probably the most important parameter defining the adsorption technique via diverse chemical interactions [13, 14]. Both carboxyl and hydroxyl groups played important roles in the immobilization of NH_3 gas in air. Molecules on the adsorbent surface were functionalized with free –COOH and –OH groups that have strong interactions with NH_3 through chemical interactions, which greatly enhanced the NH_3 gas adsorption performance [15, 16]. A similar beneficial effect for improving the ammonia removal has been described in the literature for metal-modified (Fe, Co, Cr, Mo and W) activated carbons [15, 16]. Due to the weak thermal conductivity of the activated carbon, some studies have employed expanded graphite to alter the walnut shell-based activated carbon; nonetheless, the thermal conductivity was increased largely, and thus, the regeneration efficiency of activated carbon could be improved [17, 18]. Recently, application of carbon nanomaterials such as carbon nanotubes and graphene derivatives in adsorption of heavy metals from wastewater or as lubricants modifiers has attracted a considerable attention due to their outstanding structures [19, 20].

One of the most popular commercial adsorbents is silica gel which has been popularly used as porous adsorbent for volatile organic compounds (VOCs) due to its relatively weak bonds with water as well as its large pore volume [21–23]. However, silica gel must be modified due to its limited capacity and selectivity resulting from the presence of silanol sites and low porous structure. Fu et al. [23] have prepared nano-porous carbon–silica composites using tetraethyl orthosilicate (TEOS) as the silicon source and activated carbon powder as the carbon source and detected its adsorption capacity to VOCs. Silica gel was formed through sol–gel of TEOS using ammonia solution as a basic reagent at 60 °C for 2 h. They concluded that the prepared carbon–silica composites have microporous and mesoporous structures, and thus, the adsorption capacity for n-hexane is better than that of conventional hydrophobic silica gel, and the desorption performance is superior than that of activated carbon alone. Therefore, the combination of silica particles with ACs would alternately enhance the adsorption and regeneration performance of AC adsorbents. As well as, the addition of carbon nanotubes based on their outstanding properties and morphology would improve the adsorption characteristics of ACs.

The present study is firstly aimed to investigate the possibility to produce AC-based material composites with silica and carbon nanotubes for the first time; as so as modify the surface chemistry of AC in order to render it more effective for enhancing the adsorption capacity of AC toward removal of ammonia gas (NH_3) as a pollutant in the indoor air. The second objective is to evaluate the effect of modification results for obtained composite samples toward the removal of NH_3 gas as compared to that of a commercial AC alone. In this work, three samples were tested; bare activated carbon (AC), AC modified with triethoxysilane propylamine (TEPSA) as a source of silica and carbon nanotube (CNT) to prepare (TEPSA/CNT/AC) composite and silica gel was synthesized from TEPSA to form silica nanoparticles (SiNP) with CNT over AC surface as (SiNP/CNT/AC) composite. Moreover, BET surface area, SEM, EDX, TEM and FTIR measurements were performed to estimate the properties of studied adsorbents. Langmuir and Freundlich models were applied to determine the adsorption behavior of NH_3 over these samples.

2 Materials and Methods

2.1 Materials

A commercial charcoal and orthophosphoric acid (H_3PO_4, 85 wt%, Mw = 98.0 g/mol) were supplied from Rasayan (Turkey). Triethoxysilane propylamine [TESPA] or (3-aminopropyl)triethoxysilane ($H_2N(CH_2)_3Si(OC_2H_5)_3$, Mw = 221.37 g/mol) and cetyltrimethylammonium bromide (CTAB, $C_{19}H_{42}BrN$, Mw = 364.45 g/mol) were purchased from Sigma-Aldrich. Diethylene triamine [DETA] ($(NH_2CH_2CH_2)_2NH$, Mw = 103.17 g/mol) was obtained from Thermo Scientific brand of ACROS Organics. Absolute ethanol solution (CH_3CH_2OH, 99%) was purchased from Alpha chemika. Laboratory multi-walled carbon nanotube (MWCNTs) was obtained from camphor as reported by Fathy et al. [24].

2.2 Preparation of Activated Carbon-based Composites

First, the charcoal was exposed to activation with H_3PO_4 as prescribed in the previous study [25] but with changing in the activation temperature to be 700 °C for 2 h under flowing nitrogen gas. This step was applied to increase the surface area and amount of acidic functional groups on the obtained activated carbons before modification with TESPA and MWCNTs. The obtained activated carbon was labeled as

AC. Second, about 2 g of AC was mixed with 1 mL of TESPA diluted to 20 mL of bi-distilled H_2O, heated to 50 °C under stirring for 1 h, and then, 1 mL of DETA was slowly added to mixture of AC and TESPA. After 30 min, 50 mg of MWCNT, well-dispersed in solution of 12.5-mg CTAB, 5-mL H_2O and 5-mL ethanol, was added slowly to above mixture of AC and TESPA under stirring and heating at 50 °C for 2 h. The mixture was kept overnight without heating and stirring then followed by washing with bi-distilled H_2O until the pH of filtrate becomes ~ 6, and dried at 80 °C overnight. The resulted sample was noted as TESPA/CNT/AC composite. Third, a novel modification was carried out using the same reactants with adding 2 mL of 2 M NaOH solution subsequent to the addition of DETA to form silica gel as SiNP on the surface of CNT/AC composite. Thus, the obtained composite was denoted as SiNP/CNT/AC composite.

2.3 Characterization of the Prepared Samples

The pH of surface for the obtained samples was measured after mixing 20-mg sample with 20-mL bi-distilled H_2O, heating for 30 min at 50 °C under stirring and followed by cooling. Surface morphology and compositions of the prepared samples were determined using scanning electron microscope (SEM, FEI Quanta FEG-250) combined with energy-dispersive X-ray spectroscopy (EDX). Transmission electron microscopy (TEM) was performed on a transmission electron microscope (JEOL, TEM-1230 Electron Analyzer) to identify the morphology of CNT particles distributed within AC surface. The textural properties of the obtained samples were analyzed using liquid nitrogen adsorption analysis at − 196 °C (BEL-Sorp max, MicrotracBel Crop, Japan). The external surface area and the micropore volume were determined by t-curves (a statistical thickness between 3.5 and 5.0 Å) using the Harkins–Jura equation [26]. Fourier transforms infrared spectroscopy (FTIR) spectra of samples were recorded by employing a KBr pressed disk technique (2 mg of sample and 98 mg of KBr) to give the main functional groups using FTIR 6500 spectrometer (JASCO, Japan) in the range of 400–4000 cm^{-1}.

2.4 Isotherm Adsorption of NH_3 Gas by Prepared ACs Samples

Figure 1 represents the schematic diagram of the reactor system designed for this study to evaluate the adsorption equilibrium. The reactor utilized to achieve the AC material into contact with the contaminated air was a container with a volume of 0.5 L. The main principle of the experiment involved a known volume of ammonia solvent injected into a closed reactor (in the same volume of the reactor of initial concentration, Ci), with a determined adsorbent mass (m) was introduced. After equilibrium has been reached, the gas-phase concentration (Ce) was analyzed. The adsorbent (20 mg) of prepared ACs was put in a bent tube. A defined volume of liquid NH_3 was then put in a petri dish present into the reactor at a temperature and pressure of 25 °C and 101 kPa, respectively. By slight rotation, it allows the adsorbent to be introduced into the reactor once the liquid ammonia has been evaporated. After completing NH_3 evaporation, the tube in an angled shape was rotated in order to introduce the adsorbents inside the reactor. Before starting the experiment, various NH_3 solutions were evaporated inside the empty reactor at the same experimental circumstances for evaluating the corresponding initial NH_3 concentrations. The latter NH_3 concentrations were varied from 1745 to 5079 $\mu g/m^{-3}$. The NH_3 concentration was evaluated using a calorimetric method at 460 nm by UV/VIS spectrophotometer (LKB BIOCHROM NOVASPEC 4049) [27]. The isotherms of NH_3 were determined by Langmuir and Freundlich parameter models.

2.5 Kinetic Study of Ammonia Gas Adsorption by Prepared Activated Carbon Samples

The influence of the contact time on the NH_3 removal percentage was studied at an initial NH_3 concentration of 3143 $\mu g/m^{-3}$. Finally, NH_3 gas samples were collected from reactor during the experimental period by means of gas withdrawing with a steady flow rate (1L/min) for 15 min via a bubbler including an absorbance solution (25 mL) and then analyzed.

3 Results and Discussion

3.1 Characteristics Determination of Adsorbents

The results of surface pH of obtained samples showed that AC, TESPA/CNT/AC and SiNP/CNT/AC have pH values of 4, 4.5 and 6 as listed in Table 1. Thus, the surface of AC is changed from strong acidic to slight acidic in nature confirming that the modification of AC surface with non-acidic surface groups was attained. Influence of TESPA and CNT as modifying agents on the textural properties of AC raw sample and on their surface compositions is recorded in Tables 1 and 2.

From Table 1, the prepared samples exhibited high total surface area (S_{BET}, m^2/g) and total pore volume (V_P, cm^3/g) values. However, these values are decreased after AC sample combined with TESPA and CNT components, whereas the mean pore diameter (WP, nm) value is increased from 2.31 to 3.48 nm. In addition, the t-micropore surface area ($S_{t,\ micro}$, m^2/g) and t-micropore volume ($V_{t,\ micro}$, cm^3/g) of AC are decreased upon modification confirming that

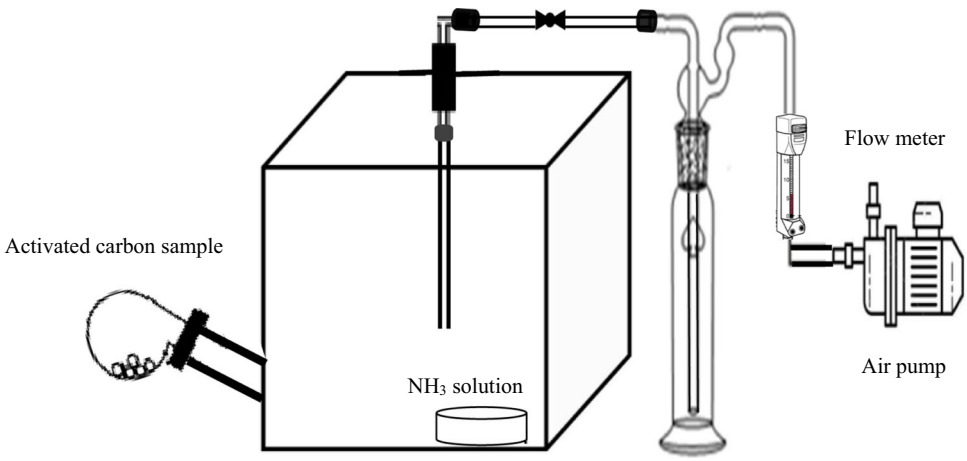

Fig. 1 Schematic diagram of experimental system designed for the removal of ammonia from the indoor air using prepared AC-based materials

Table 1 Porous characteristics of the prepared samples as accounted from N_2 adsorption at –196 °C (total surface area (S_{BET}, m^2/g), total pore volume (V_P, cm^3/g), mean pore diameter (WP, nm), t-micropore surface area ($S_{t,\,micro}$, m^2/g) and t-micropore volume ($V_{t,\,micro}$, cm^3/g))

Samples	pH	S_{BET} (m^2/g)	V_P (cm^3/g)	WP (nm)	$S_{t,\,micro}$ (m^2/g)	$V_{t,\,micro}$ (cm^3/g)	$V_{t,\,micro}/V_P$, %
AC	4	1202	0.695	2.31	1093	0.499	71.8
TESPA/CNT/AC	4.5	442	0.315	2.85	355	0.212	67.3
SiNP/CNT/AC	6	350	0.304	3.48	229	0.156	51.3

Table 2 Element compositions of the prepared samples according to EDX analysis

Samples	EDX analysis				
	C	O	Si	N	P
AC	72	23	0	0.50	4.50
TESPA/CNT/AC	76	18	0.95	0.75	4.30
SiNP/CNT/AC	77	16.5	2.10	0.90	3.50

these components covered or retained inside the micropores of AC sample, and thus, the microporosity is decreased considerably from 71.8 to 51.3%, although the mesoporosity is increased consequently. Clearly, the deposited silica nanoparticles (SiNP) in silica gel formed within AC surface using NaOH could be diffused into the bulk of AC through the internal pores giving rise to a decrease in the internal porosity as shown in Table 1.

EDX analysis indicated that the AC sample composed of C, O, N and P while other samples contained Si element which is varied from 0.95% in TESPA/CNT/AC to 2.10% in SiNP/CNT/AC. Also, the content of N element is increased as a result of TESPA and DETA reagents containing amino groups in their chemical structures. For the preparation of SiNP/CNT/AC sample, the applied approach is a simple and novel to combine between SiNP and CNT components over AC surface in order to improve the adsorption of ammonia gas.

SEM images of the prepared samples are depicted in Fig. 2. Obviously, the samples exhibit the same surface morphology regarding to the structure of AC. They are composed of irregular grains with cavities of different pores which are small, transitional and large pores of different shapes as shown in its micrograph. However, after modification of AC with after using TESPA and CNT components, a large number of these cavities are blocked. Bundles of CNTs are not observed in SEM pictures of TESPA/CNT/AC and SiNP/CNT/AC samples using both magnifications at low (100 μm, Fig. 2B and C). Nevertheless, TEM analysis was performed to identify the morphology of CNT particles distributed within AC. Straight bundles within AC structure that covered by layers of SiNP (black shadow) have tubes with diameters ranging from 50 to 122 nm at high magnification of 1 μm as illustrated in Fig. 3.

To examine the surface functional groups created along the combination of TESPA and CNT or SiNP and CNT over AC sample, FTIR spectrum was run and recorded at range 4000–400 cm^{-1} as shown in Fig. 4. Assignments of the

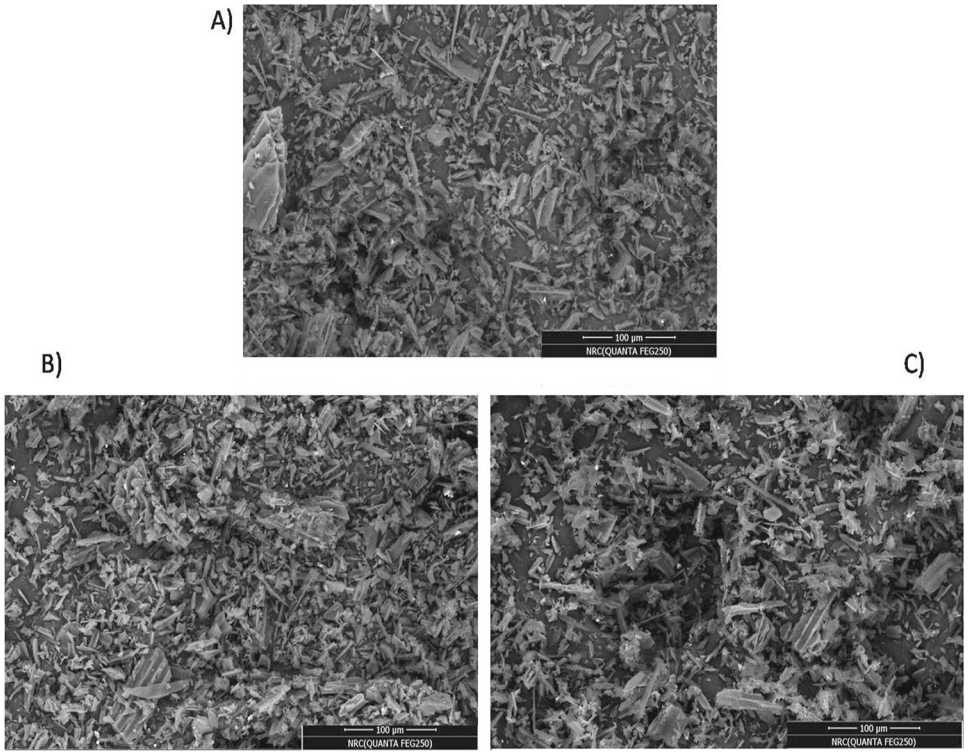

Fig. 2 SEM images of the samples **A** AC, **B** TESPA/CNT/AC and **C** SiNP/CNT/AC

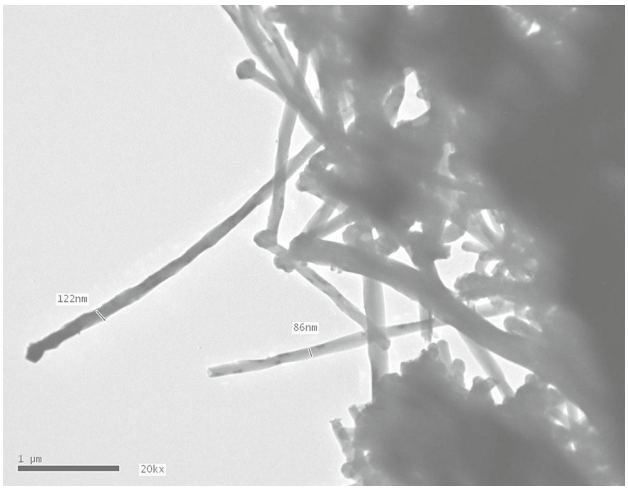

Fig. 3 TEM image of SiNP/CNT/AC at high magnification 1 µm

resulted absorption bands are listed in Table 3. As reported before, the appearance of siloxane and silanol groups in FTIR can be inferred to the formation of silica gel [23, 28–30]. FTIR spectrum of parent AC sample showed five absorption band characteristics at the following regions: 3430.7, 2078.9, 1635.3/1619.5, 1384.6 and 715–400 cm^{-1} with higher absorbance intensities than that of other samples. After the addition of TESPA/CNT or SiNP/CNT, the absorbance intensity of those bands for AC is decreased with a shifting in their wavenumbers (cm^{-1}). This observation is followed by appearing two broad absorption bands located between 971 and 679 cm^{-1} besides 1053 and 983 cm^{-1} for TESPA/CNT/AC and SiNP/CNT/AC. Thus, as a result of these FTIR findings, the use of NaOH with TESPA converts considerably TESPA over CNT/AC to silanol groups as SiNP which precipitated in the presence of alkali agent rather than use TESPA only as source of Si particles as determined by increasing in its surface pH from 4.5 to ~ 6. This strategy achieved better performance in the adsorption efficiency of NH3 than that obtained using AC and TESPA/CNT/AC samples.

3.2 Kinetic Adsorption of Ammonia Gas Using the Prepared ACs Samples

Figure 5 exhibits the obtained results for the NH_3 gas adsorption as a function of the time onto the ACs surface, TESPA/CNT/AC and SiNP/CNT/AC samples. As depicted in this figure, during the adsorption process for all prepared AC-based samples, the NH_3 gas behaves the same trend and can be divided into three stages: First stage, a rapid adsorption phase was reached, where the NH_3 gas concentration was declined very rapidly during a contact time period of nearly 10 h, then slow adsorption phase: Where the NH_3 gas concentration was decreased very slowly after almost 10 h, and finally, a steady-state phase in which the equilibrium was achieved. As well-known, the adsorption process is surface phenomena that highly depend on the properties

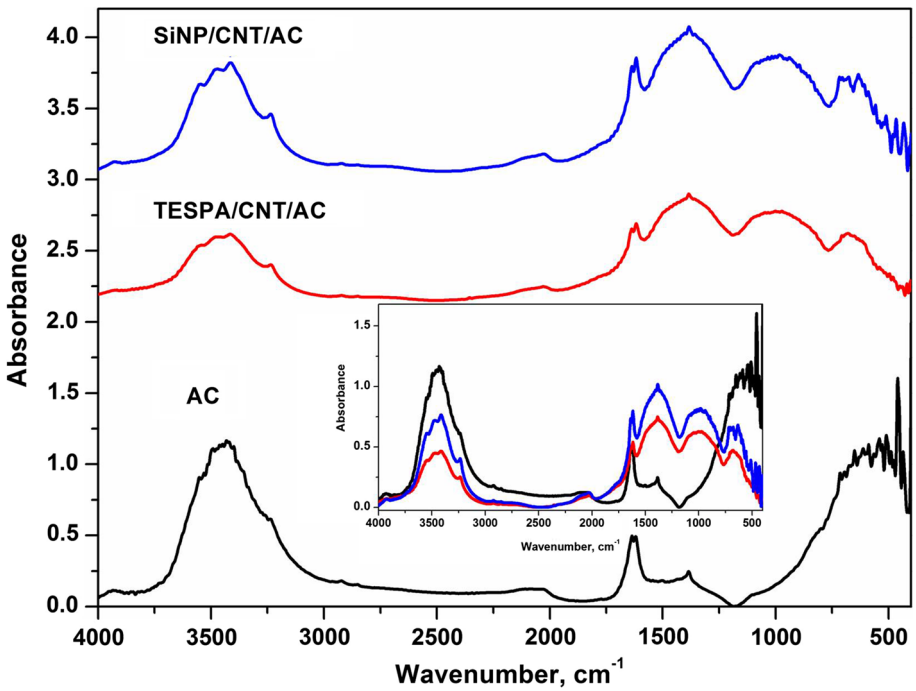

Fig. 4 FTIR spectra of the prepared adsorbents

Table 3 FTIR absorption band assignments in the prepared samples

Absorption bands, wavenumber cm^{-1}			Peak assignments
AC	TESPA/CNT/AC	SiNP/CNT/AC	
3430.7	3415.5	3413.3	O–H stretching vibration in benzene ring and H_2O
2925, 2848	2923, 2848	2923, 2846	C–H stretching vibration (asymmetric and symmetric)
2078.9	2029.7	2028.7	N–H in NH_3 amine vibration
1635.3 1619.5	1637.3 1617.5	1637.3 1617.5	O–H bending vibration, Si–NH (1637 cm^{-1}) ν(C = C) and ν(C = O) of inter-ring chain
1384	1379	1389	C = O stretching symmetric in COO^-
– 	971 679	1053 983	Si–OH silanol and Si–O–Si siloxane stretching vibration C–Si–O stretching vibration
780–433	776–462	790–482	C–H in all samples with C–Si stretching and bending in presence of TESPA and SiNP

of surface and functional groups [31]. This idea can be interpreted as follows: (1) Firstly, the quantities of free adsorption sites will reduce as time augments, (2) secondly, at the early rapid stage of NH_3 gas adsorption onto the ACs adsorbents, it mainly includes the surface diffusion and (3) as time augments, the active sites on ACs surfaces will be saturated; meanwhile, these will lead to a slow rate of the gas pollutant adsorption. The surface adsorption is generally very fast with the early time of adsorption as previously reported [32]. Similarly, Rashidi et al. [33] cited that rapid adsorption is governed by the surface area of adsorbents that are responsible for the interaction with the target pollutant gas over time. Also, the adsorption rate was noticed to be decreased due to a reduction in the active sites that may delay the adsorption process [33]. Moreover, the initial adsorption step is rapid due to the adsorption of the target pollutant on the external adsorbent surfaces, and then with time, a slower adsorption was attained which is attributed to the slow diffusion of pollutants into the adsorbent pores since the majority of the available external active sites has already been occupied at the initial step [34].

The functional groups in the adsorbents characterized by the FTIR analysis (Fig. 4 and Table 3) revealed the presence of a carbonyl group (C = O) and hydroxyl group (− OH) at 1637 cm^{-1} and a hydroxyl stretching vibration at nearly 3415 cm^{-1} (− OH), indicating the presence of carboxyl groups (− COOH) in the samples of TESPA/CNT/AC and SiNP/CNT/AC as compared to the parent AC sample, which possess higher electron affinity and high ability to improve the NH_3 reactivity on the adsorbent surface [35].

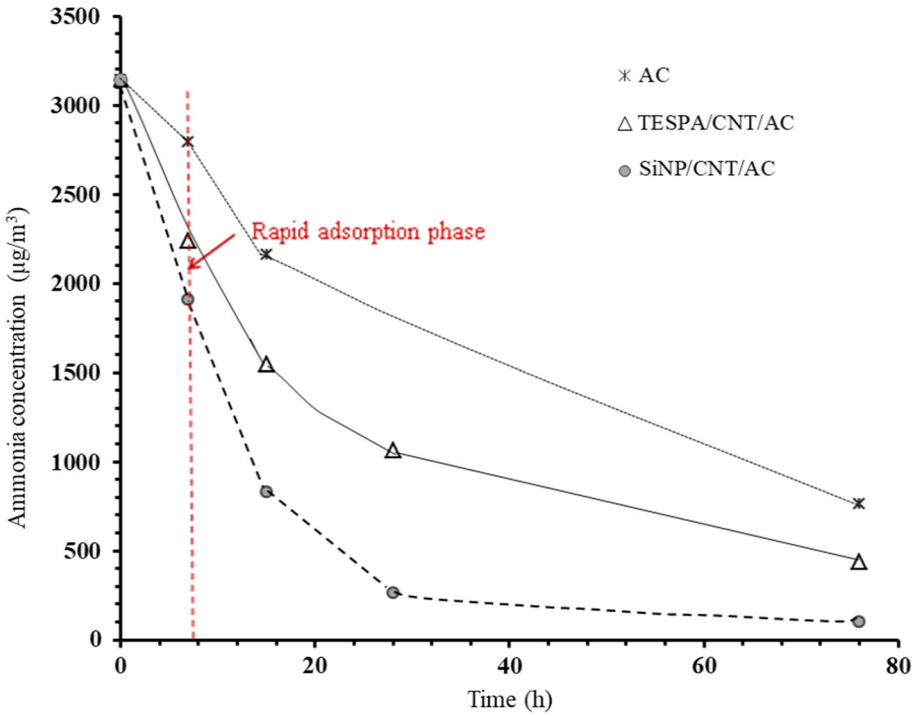

Fig. 5 Uptake of ammonia gas concentration using the new AC-based material samples (AC, TESPA/CNT/AC and SiNP/CNT/AC)

SiNP/CNT/AC has a higher number of Si–OH silanol and Si–O–Si siloxane sites than that of TESPA/CNT/AC sample as seen in FTIR analysis, leading to an adsorption of NH_3 much more than that of both TESPA/CNT/AC and AC, despite the higher surface area of the latter samples, TESPA/CNT/AC and AC. Furthermore, this confirms that the presence of SiNP is responsible for the enhancement in NH_3 adsorption on the silica sites which has been assigned as vibrations of Si–O-Si, Si–OH, Si-NH and Si–C groups. Such groups may lead to the chemisorption of NH_3–hydrogen to the − OH groups on the silica surface. These findings are confirmed in good agreement with the SEM–EDX results, and the bulk surface Si content of SiNP/CNT/AC appeared to be 2.1% as compared to 0.9% and zero for TESPA/CNT/AC and AC samples, respectively. Moreover, SiNP/CNT/AC exhibited a high-speed removal reaction and the improvement in kinetics (i.e., high adsorption rate) which attributed to its enhanced portions of mesoporous structure in CNT, where the mean pore diameter value was augmented from 2.31 to 3.48 nm, promoting the diffusion rate of NH_3.

3.3 Ammonia Gas Adsorption Isotherms by Prepared ACs Samples

Comparison between the adsorption behavior of the three prepared AC-based samples (AC, TESPA/CNT/AC and SiNP/CNT/AC) is presented in Fig. 6. The results showed that SiNP/CNT/AC has the strongest adsorption removal of NH_3 gas followed by TESPA/CNT/AC and then AC sample within the investigated range of NH_3 concentrations. These results cannot be interpreted by the BET surface area of the samples, where AC sample has the highest surface area. Indeed, this behavior may be due to the presence of hydroxyl, carboxyl and silica functional groups present on each modified sample surface. The NH_3 gas has a basic character; hence, the adsorption removal will be increased by the presence of acidic functional groups on the adsorbent surface. The influence of surface chemistry, nature and amount of O-containing functional groups highly affect the NH_3 removal. The experiments of NH_3 adsorption showed that the modification of the original AC, including the incorporation of O-surface groups, strongly improves the NH_3 adsorption behavior. Apparently, there is a direct relationship between the NH_3 total adsorption capacity and the amount of the most acidic O-surface functional groups [36].

In comparison with the results of NH_3 isotherms in quantitative patterns, the data were evaluated by two principal models (Langmuir and Freundlich) and the obtained constants of kinetic parameters are summarized in Table 4. The R^2 (correlation coefficient square) parameters of both models at 25 °C confirmed that the empirical equation of Freundlich model is more suitable than that of Langmuir in describing the NH_3 gas adsorption and fit well the data for all prepared AC-based samples, confirming that adsorption process is chemisorption also.

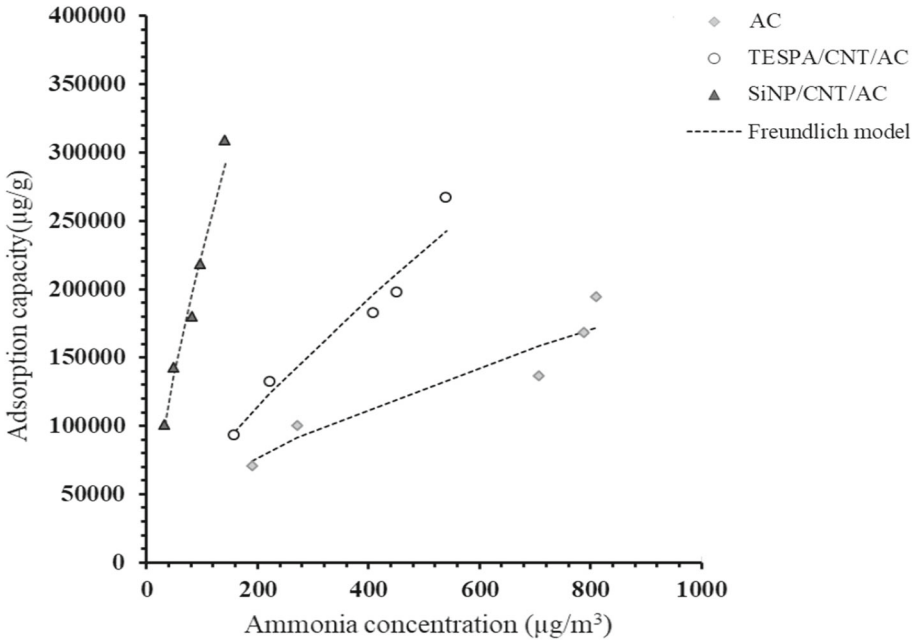

Fig. 6 Experimental equilibrium data of NH_3 gas adsorption isotherms using AC-based materials (AC, TESPA/CNT/AC and SiNP/CNT/AC) and the predicted theoretical Freundlich isotherm

Table 4 Parameters of Langmuir and Freundlich models for the NH_3 adsorption using three AC-based material samples (AC, TESPA/CNT/AC and SiNP/CNT/AC) at 25 °C

ACs based materials	Langmuir model			Freundlich model		
	q_{max} ($\mu g.g^{-1}$)	K_L $m^3.\mu g^{-1}$	R^2	n	K_F ($\mu g.g^{-1}$) ($m^3.\mu g^{-1}$)$^{1/n}$	R^2
SiNP/CNT/AC	1000000	0.0033	0.76	1.4	8076	0.98
TESPA/CNT/AC	1000000	0.0006	0.63	1.4	2035	0.96
AC	333333	0.0015	0.81	1.8	3625	0.93

q_{max} is the monolayer adsorption capacity ($\mu g\ g^{-1}$) and K_L ($m^3\ \mu g^{-1}$) is the Langmuir adsorption equilibrium constant calculated from the equation: $C_e/q_e = 1/K_L q_{max} + 1/q_{max}\ C_e$; K_F ($\mu g\ g^{-1}$) ($m^3\ \mu g^{-1}$)1/n is roughly an indicator of the adsorption capacity and n is the adsorption intensity and derived from the equation: $\log C_e = \log K_F + 1/n \log C_e$ R^2 is a correlation coefficient for straight line of each equation

Figure 6 exhibits the experimental equilibrium data for the isotherms of NH_3 adsorption using the three AC-based samples and the predicted theoretical Freundlich isotherm. It was observed that the isotherms of NH_3 gas for all prepared ACs samples were of type II. The latter revealed the formation of multiple layers of NH_3 adsorbed successively to further interactions between the NH_3 gas molecules and active sites obtained on the surface prepared samples. Also, the possibilities of forming these layers typically coincide with the mesoporous characters of the prepared AC samples. The findings obtained in Fig. 6 confirmed that the Freundlich model was consistent with the NH_3 adsorption data for all prepared AC-based materials. Freundlich model constants indicated that the SiNP/CNT/AC sample possesses the highest K_F value compared to those of TESPA/CNT/AC and AC samples (Table 4); thus, this result indicates that the adsorption capacity of SiNP/CNT/AC exceeds that of TESPA/CNT/AC and AC samples. The value of n also assumes higher adsorption intensities in the prepared AC samples. In general, the values of $n > 1$ represent favorable adsorption of the target pollutant by the studied AC-based samples.

Figure 7 shows that at the adsorption process end, almost 97% NH_3 gas pollutant was adsorbed via SiNP/CNT/AC, whereas nearly 86% was removed by TESPA/CNT/AC, and only 75% adsorbed NH_3 gas was achieved by AC sample. Emphatically, SiNP/CNT/AC exhibited the highest NH_3 adsorption capacity, although SiNP/CNT/AC possessed a lower specific surface area than both TESPA/CNT/AC and AC. These results indicated that the NH_3 adsorption capacity has a weak interrelation with the specific surface area and expect an extra important factor can act between the solid and the NH_3 gas adsorption reaction. Therefore, using a modified SiNP/CNT/AC showed a preferential adsorption pathway via Brønsted and Lewis acid centers existed in the carbon surface

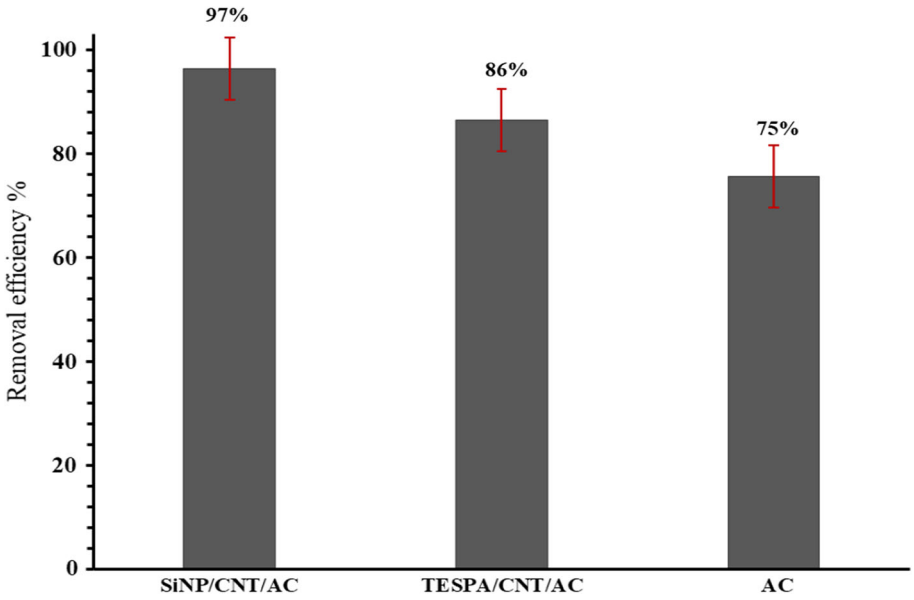

Fig. 7 Ammonia gas removal efficiency using the prepared AC-based material samples (AC, TESPA/CNT/AC and SiNP/CNT/AC)

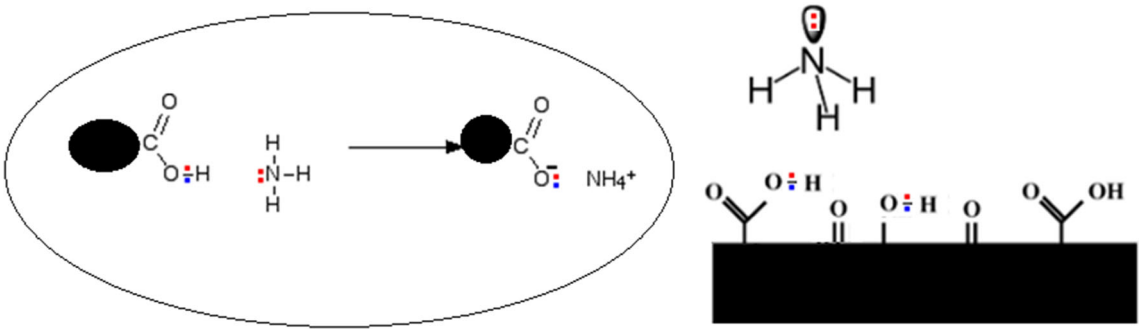

Fig. 8 Suggested reaction of NH_3 gas as an electron donor and the main acidic functionality groups on the surface of carbon materials via the adsorption process

after modification. FTIR analyses of the samples confirmed the presence of acid sites on the solid layers that interact together with NH_3 gas, through the lone pair of electrons.

Similarly, Lyobe et al. [37] found that many acidic groups on the adsorbent surfaces possess higher chemical adsorption potentials for NH_3 gas at 20 °C. Both carboxylic and hydroxyl groups played critical roles in immobilizing of NH_3 gas from the air. The molecules on the adsorbents surface functionalized by free –COOH and –OH groups, which had strong interactions with NH_3 by chemical interaction, thus greatly improving the adsorption performance for NH_3 gas. Furthermore, the previous studies reported in the literature indicated that the surface chemistry is probably the most critical factor controlling the total adsorption capacity [13, 14]. Vigorous adsorption of NH_3 gas on acidic functional groups (–COOH groups) is well previously recorded [38]. Figure 8 shows the suggested reaction of NH_3 gas as an electron donor and the main functional groups (− COOH and − OH groups) on the surface of carbon materials via the adsorption process, in which NH_3 gas, being basic, reacts with sub-acidic –COOH and –OH groups, resulting in a nucleophile attack on the carbon surface.

Adsorption removal of contaminants by conventional adsorbents is mainly due to their porous structure and weak hydrogen bonding, which carries the risk of re-release of contaminants [13]. However, we hypothesize that the NH_3 molecules are tightly bound to the acidic sites on the surface of the new adsorbent material, thus reducing the risk of NH_3 re-release. This work may provide a viable way for developing promising adsorbents for removing NH_3 gas from the air. Therefore, in order to recycle the adsorbent, we thought that a regeneration operation of adsorbents would be necessary to be studied in forthcoming future, by coupling the adsorption and advanced oxidation processes to regenerate the adsorbent after catalytic decomposition of the adsorbed contaminants [14].

For comparison, Table 5 shows the comparison between the amounts of NH_3 gas adsorbed on the prepared AC-based materials in the present work and previously reported amounts using different adsorbents by Yeom et al. [38].

Table 5 Comparison of NH_3 gas adsorption capacities between prepared activated carbon-based materials and various adsorbents

Adsorbents	Adsorption capacity of NH_3 gas (mg g^{-1})	References
SiNP/CNT/AC	300	Present work
TESPA/CNT/AC	267	Present work
AC	194	Present work
Zeolite (Ze, < 45 μm, CAS#1318-02-1)	43.8	[38]
Mesoporous alumina	214	
Activated carbon (AC, 100 mesh)	45.8	
Silica	33	

As can be seen, the NH_3 gas adsorption capacities of the prepared AC-based materials are of the most significant magnitude as compared to those observed using other adsorbents. Generally, the gaseous NH_3 adsorption capacities of all adsorbents ranged from 30 to 300 mg g^{-1} (Table 5). Therefore, the obtained AC-based composites are very promising candidate for the removal of NH_3 gas from indoor air.

4 Conclusions

Novel adsorbents were synthesized by modification of derived activated carbon (AC) from commercial charcoal with triethoxysilane propylamine (TEPSA) and carbon nanotube (CNT). Combination of silica nanoparticles and CNT over AC surface led to a significant increase in the active adsorption sites such as acidic functional groups, siloxane and silanol accompanied with mesopores inside CNT and to a substantial decrease in the total surface area and total pore volume. These findings suggested that the adsorption of NH_3 gas is mainly related to acidic adsorption sites and accessible mesopores and is not to total surface area. Furthermore, the adsorption capacity of SiNP/CNT/AC is higher than that of TESPA/CNT/AC and AC that is owing to high amount of silica nanoparticles. From these results, the prepared carbon–nanosilica composites with CNT strongly enhanced the adsorption performance of AC, and thus, they can candidate as effective adsorbents in ammonia removal and used as a new alternative for solving air pollution.

Acknowledgements Authors are thankful to the National Research Center, Egypt, for supporting this work with technical facilities including chemicals and equipment.

Author contributions All the authors contributed equally in this work.

Funding Open access funding provided by The Science, Technology & Innovation Funding Authority (STDF) in cooperation with The Egyptian Knowledge Bank (EKB). The author(s) received no specific financial funding for this work.

Declarations

Conflict of interestt The authors declare that they have no known competing financial interests or personal relationships that could have appeared to influence the work reported in this paper.

References

1. Behera, S.N.; Sharma, M.; Aneja, V.P.; Balasubramanian, R.: Ammonia in the atmosphere: a review on emission sources, atmospheric chemistry and deposition on terrestrial bodies. Environ. Sci. Pollut. Res. **20**, 8092–8131 (2013)
2. Chang, Y.H.: Non-agricultural ammonia emissions in urban China. Atmos. Chem. Phys. Discuss. **14**, 8495–8531 (2014)
3. Manuzon, R.B.; Zhao, L.Y.; Keener, H.M.; Darr, M.J.: A prototype acid spray scrubber for absorbing ammonia emissions from exhaust fans of animal buildings. Am Soc Agri Biol Eng **50**, 1395–1407 (2007)
4. Liu, Y.; Li, X.-S.; Liu, J.-L.; Shi, C.; Zhu, X.; Zhu, A.-M.; Jang, B.W.-L.: Ozone catalytic oxidation for ammonia removal from simulated air at room temperature, Catal. Sci. Technol. **5**, 2227–2237 (2015)
5. Ashtari, A.K.; Majd, A.M.S.; Riskowski, G.L.; Mukhtar, S.; Zhao, L.: Removing ammonia from air with a constant pH, slightly acidic water spray wet scrubber using recycled scrubbing solution. Front. Environ. Sci. Eng. **10**, 3 (2016)
6. S. J. Blonigen, A. G. Fassbender, R. D. Litt, B. F. Monzyk, R. Neff, Method for ammonia removal from waste streams, US patent n 6,558,643 (2003)1–18.
7. Mohamed, E.F.; Ahmed, S.A.S.; Abdel-Latif, N.M.; El-Mekawy, A.: Air purifier devices based on adsorbents produced from valorization of different environmental hazardous materials for ammonia gas control. RSC Adv. **6**, 57284–57292 (2016)
8. Gebreegziabher, T.B.; Wang, S.; Nam, H.: Adsorption of H_2S, NH_3 and TMA from indoor air using porous corncob activated carbon: Isotherm and kinetics study. J. Environ. Chem. Eng. **7**, 103234 (2019)
9. Hsieh, C.-C.; Tsai, J.-S.; Chang, J.-R.: Effects of moisture on NH_3 capture using activated carbon and acidic porous polymer modified by impregnation with H_3PO_4: Sorbent material characterized by synchrotron XRPD and FT-IR. Materials **15**(784), 1–14 (2022)

10. Huang, C.-C.; Li, H.-S.; Chen, C.-H.: Effect of surface acidic oxides of activated carbon on adsorption of ammonia. J. Hazard. Mater. **159**, 523–527 (2008)
11. Kim, B.-J.; Park, S.-J.: Effect of carbonyl group formation on ammonia adsorption of porous carbon surfaces. J. Colloid Interface Sci. **311**, 311–314 (2007)
12. Le Leuch, L.M.; Bandosz, T.J.: The role of water and surface acidity on the reactive adsorption of ammonia on modified activated carbons. Carbon **45**, 568–578 (2007)
13. Ali, I.; Burakova, I.; Galunin, E.; Burakov, A., et al.: High-speed and high-capacity removal of methyl orange and malachite green in water using newly developed mesoporous carbon: kinetic and isotherm studies. ACS Omega **4**, 19293–19306 (2019)
14. Ali, I.; Kon'kova, T.; Kasianov, V.; Rysev, A.; Panglisch, S.; Mbianda, X.Y.; Habila, M.A.; Al Masoud, N.: Preparation and characterization of nano-structured modified montmorillonite for dioxidine antibacterial drug removal in water. J. Mol. Liq. **331**, 115770 (2021)
15. Petit, C.; Bandosz, T.J.: Role of surface heterogeneity in the removal of ammonia from air on micro/mesoporous activated carbons modified with molybdenum and tungsten oxides. Microp. Mesop. Mater. **118**, 61–67 (2009)
16. Bandosz, T.J.; Petit, C.: On the reactive adsorption of ammonia on activated carbons modified by impregnation with inorganic compounds. J. Colloid Interface Sci. **338**, 329–345 (2009)
17. Kuwagaki, H.; Meguro, T.; Tatami, J.; Tamura, K.: An improvement of thermal conduction of activated carbon by adding graphite. J. Mater. Sci. **38**, 3279–3284 (2003)
18. Wang, L.W.; Metcalf, S.J.; Critoph, R.E.; Thorpeb, R.; Tamainot-Telto, Z.: Development of thermal conductive consolidated activated carbon for adsorption refrigeration. Carbon **50**, 977–986 (2012)
19. Ali, I.; Burakov, A.E.; Melezhik, A.V.; Babkin, A.V.; Burakova, I.V.; Neskomornaya, E.A.; Galunin, E.V.; Tkachev, A.G.; Kuznetso, D.V.: Removal of copper (II) and zinc (II) ions in water on a newly synthesized polyhydroquinone/graphene nanocomposite material: kinetics, thermodynamics and mechanism. Chem. Select **4**, 12708–12718 (2019)
20. Ali, I.; Basheer, A.A.; Kucherova, A.; Memetov, N.; Pasko, T.; Ovchinnikov, K.; Pershin, V.; Kuznetsov, D.; Galunin, E.; Grachev, V.; Tkachev, A.: Advances in carbon nanomaterials as lubricants modifiers. J. Mol. Liq. **279**, 251–266 (2019)
21. Wang, Y.; Huang, W.; Lv, Y.; Wang, W.; Wang, Y.: Investigation of modified hydrophobic silica gel for gasoline vapor adsorption and desorption. Chin. J. Environ. Eng. **9**, 855–891 (2015)
22. Huang, W.; Bai, J.; Shen, Y.: Composites adsorbent of activated and hydrophobic silica gel for gasoline vapor recovery. Chem. Eng. N. Y. **39**, 38–41 (2011)
23. Fu, L.; Zhu, J.; Huang, W.; Fang, J.; Sun, X.; Wang, X.; Liao, K.: Preparation of nano-porous carbon-silica composites and its adsorption capacity to volatile organic compounds. Processes **8**(3), 372 (2020). https://doi.org/10.3390/pr8030372
24. Fathy, N.A.; El-Khouly, S.M.; El-Shafey, O.: Modified carbon nanostructures obtained from sugarcane bagasse hydrochar for treating chromium-polluted water. CAC **17**(7), 975–988 (2021). https://doi.org/10.2174/1573411016666200106101921
25. Mohamed, G.M.; Rashwan, W.E.; Fathy, N.A.; Sayed Ahmed, S.A.: Effect of nitrogen functionalization on the adsorption performance of commercial charcoal activated with phosphoric acid. Des. Water Treat. **148**, 178–187 (2019)
26. Buttersack, C.; Möllmer, J.; Hofmann, J.; Gläser, R.: Determination of micropore volume and external surface of zeolites. Microporous Mesoporous Mater. **236**, 63–70 (2016)
27. Harrison, M.; Perry, R.: Handbook of air pollution analysis, 2nd edn. Chapman and Hall, London, New York (1986)
28. Shi, F.; Wang, L.; Liu, J.: Synthesis and characterization of silica aerogels by a novel fast ambient pressure drying process. Mater. Lett. **60**, 3718–3722 (2006)
29. Jabbour, J.; Calas, S.; Gatti, S.; Kribich, R.K.; Myara, M.; Pille, G.; Ettienne, P.; Moreau, Y.: Characterization by IR spectroscopy of an hybrid sol–gel material used for photonic devices fabrication. J. Non-Cryst. Solids **354**, 651–658 (2008)
30. Widjonarko, D.M.; Jumina, I.; Nuryono, K.: Phosphonate modified silica for adsorption of Co(II), Ni(II), Cu(II) and Zn(II). Indo. J. Chem. **14**(2), 143–151 (2014)
31. Chatterjee, R.; Sajjadi, B.; Chane, W.; Mattern, D.L.; Hamner, N.; Raman, V.; Dorris, A.: Effect of pyrolysis temperature on physicochemical properties and acoustic-based amination of biochar for efficient CO_2 adsorption. Front. Energy Res. **8**, 85 (2020)
32. Plazinski, W.; Dziuba, J.; Rudzinski, W.: Modeling of sorption kinetics: the pseudo-second order equation and the sorbate intraparticle diffusivity. Adsorption **19**, 1055–1064 (2013)
33. Rashidi, N.A.; Yusup, S.; Lam, H.L.: Kinetic studies on carbon dioxide capture using activated carbon. Chem. Eng. Trans. **35**, 361–366 (2013)
34. Liu, Q.-X.; Zhou, Y.-R.; Wang, M.; Zhang, Q.; Ji, T.; Chen, T.-Y.; Yu, D.-C.: Adsorption of methylene blue from aqueous solution onto viscose-based activated carbon fiber felts: kinetics and equilibrium studies. Adsorp. Sci. Technol. **37**, 312–332 (2019)
35. Miyauchi, M.; Ohba, T.: Enhancement of NH_3 and water adsorption by introducing electron-withdrawing groups with maintenance of pore structures. Adsorption **25**, 87–94 (2019)
36. Choi, J.H.; Jang, J.T.; Yun, S.H.; Jo, W.H.; Lim, S.S.; Park, J.H.; Chun, S.; Lee, J.-H.; Yoon, Y.: Efficient removal of ammonia by hierarchically porous carbons from a CO_2 capture process. Chem. Eng. Technol. **43**, 2031–2040 (2020)
37. Lyobe, T.; Asada, T.; Kawata, K.; Oikawa, K.: Comparison of removal efficiencies for ammonia and amine gases between woody charcoal and activated carbon. J. Health Sci. **50**, 148–153 (2004)
38. Yeom, C.; Kim, Y.: Adsorption of ammonia using mesoporous alumina prepared by a templating method. Environ. Eng. Res. **22**, 401–406 (2017)